Non-perturbative solution of the time-dependent Schrödinger equation describing H_2 in intense short laser pulses

2005 J. Phys. B: At. Mol. Opt. Phys. 38 3973

(http://iopscience.iop.org/0953-4075/38/22/005)

INSTITUTE OF PHYSICS PUBLISHING JOURNAL OF PHYSICS B: ATOMIC, MOLECULAR AND OPTICAL PHYSICS

J. Phys. B: At. Mol. Opt. Phys. **38** (2005) 3973–3985 doi:10.1088/0953-4075/38/22/005

Non-perturbative solution of the time-dependent Schrödinger equation describing H_2 in intense short laser pulses

Manohar Awasthi, Yulian V Vanne and Alejandro Saenz

Humboldt-Universität zu Berlin, Institut für Physik, AG Moderne Optik, Hausvogteiplatz 5-7, D-10117 Berlin, Germany

Received 24 August 2005
Published 25 October 2005
Online at stacks.iop.org/JPhysB/38/3973

Abstract

A method for solving the time-dependent Schrödinger equation describing the electronic motion of molecular hydrogen exposed to very short intense laser pulses has been developed. The fully correlated three-dimensional time-dependent electronic wavefunction is expressed in terms of field-free wavefunctions. These are obtained from a configuration-interaction calculation where the one-electron basis functions are built from *B* splines. The reliability of the method is tested by comparing results in the low-intensity regime to the prediction of lowest order perturbation theory. The onset of non-perturbative effects is shown for higher intensities and the validity of the single-active electron approximation is briefly discussed. Finally, the ability of the method to calculate photoelectron spectra including above-threshold-ionization peaks is demonstrated.

(Some figures in this article are in colour only in the electronic version)

1. Introduction

The field of laser-matter interaction has recently gained even more momentum due to the development of ultrashort intense laser pulses, now extending into the sub-femtosecond regime [1–3]. Additional interest is stimulated by the (planned) new lasers (or more intense sources for high harmonics) extending the range of available photon frequencies to the vacuum UV or even to the x-ray regime [4, 5]. These new experimental developments are very likely to produce new puzzling results that will demand theoretical explanation. Already now there exist a number of experimental data even for very small atomic or molecular systems that await their full theoretical understanding.

Molecular hydrogen plays a prominent role for experiments on laser-matter interaction, because it is from the theoretical point of view the simplest molecular system that contains more than a single electron. Compared to H_2^+ (that in addition lacks the many-electron aspect)

H_2 is also much easier to handle experimentally. Therefore, a plethora of experimental data exists for H_2 exposed to laser fields (see [6] and references therein). Despite being almost the simplest molecule, attempts to describe the behaviour of H_2 in short laser pulses in a non-simplified manner are very sparse. So far, practically all experiments were analysed by assuming tunnel ionization. The corresponding ionization rates were obtained from simple atomic tunnelling models such as the Ammosov–Delone–Krainov (ADK) theory. Only very recently an extension of the atomic ADK model incorporating the molecular structure (MO-ADK) was proposed and applied for the interpretation of experimental results [7, 8]. An alternative approach has been proposed that is also based on the quasi-static approximation but adopts *ab initio* static ionization rates and time-averaged field-distorted Born–Oppenheimer potentials. It was successfully used for predicting the vibrational final-state distribution of H_2^+ formed in laser-induced ionization of H_2 [9]. Due to the good agreement between the molecular *ab initio* results and the atomic ADK model in the relevant intensity regime, the ADK model was in fact used in the calculation for convenience reasons.

The quasi-static approximations (either using simple tunnel-ionization models or *ab initio* dc rates) are valid only for high intensities and low photon frequencies. In the opposite limit (low intensity and high photon frequency), the ionization process may be described by the lowest order perturbation theory (LOPT). An advantage of LOPT is that it introduces well-defined approximations and can systematically be improved on. However, LOPT calculations are computationally demanding and thus the first systematic and correlated calculations of non-resonant LOPT ionization rates for H_2 have only recently been performed [10].

Another popular approach is the Keldysh–Faisal–Reiss (KFR) theory, also known as strong-field approximation (SFA). This approach can alternatively be viewed as being the first term of an intense-field *S*-matrix theory (ISMT). While higher order terms have been discussed for atoms [11], the application to molecules was so far limited to the first-order term. This corresponds to the traditional strong-field approximation in which the process is described as a transition from a field-free initial state to a final Volkov state ignoring thus the Coulomb interaction of the ejected electron with the remaining ion. Molecular effects have recently also been incorporated [12] into the model. However, there is some dispute about the use of length or velocity gauge and the applicability of a Coulomb-correction factor [13].

All the models discussed above are intrinsically adiabatic models (at least with respect to the electronic motion) and thus effects due to the shortness of ultrashort laser pulses are not taken into account. In addition, all models have their drawbacks even within their (assumed) range of applicability. While LOPT rates are comparatively difficult to calculate (requiring a summation/integration over, in principle, all intermediate field-free states), the most easily obtained ADK rate does not consider any photon-frequency dependence. The SFA calculation requires the evaluation of the field-free ground-state wavefunction and its overlap with the Volkov state. It incorporates some frequency dependence (especially channel-closing aspects), but does not contain any information on the possible influence of (intermediate) resonances. This is on the other hand considered in LOPT. Since a direct comparison with experimental data is often difficult and in addition requires usually an averaging over many parameters (the spatio-temporal shape of the laser pulse that may even not be known very precisely), a direct comparison to full solutions of the time-dependent Schrödinger equation (TDSE) is desirable. A further advantage of such a comparison is the ability to compare results at a well-defined level of approximation. For example, the exact influence of nuclear motion (rotation and vibration) is still rather unclear (and depends on the experimental parameters like pulse length). While the verification of a model by means of a comparison to experimental results has to simulate the complete process, a theoretical comparison can be performed by concentrating on a single

(artificially fixed) nuclear configuration relative to the laser polarization (and using identical laser-pulse parameters).

However, solving the TDSE even within the fixed-nuclei approximation is a very demanding task. Thus, most of the solutions of the TDSE of molecules were restricted to the single-electron system H_2^+, and even there often one- or two-dimensional model Hamiltonians were applied. The same idea of reduced symmetry has also been utilized for H_2 [14] and is still popular, see, e.g., [15]. A full three-dimensional approach was introduced in [16]. A special grid-technique allowed the efficient solution of the TDSE, but only for a parallel orientation of the laser polarization and the molecular axis (reducing the dimensionality due to cylindrical symmetry). An intrinsic problem of grid methods is the non-unique definition of the ionization yield that is usually encountered.

In this work, an alternative approach for solving the TDSE describing molecular hydrogen exposed to short intense laser pulses was implemented. It is based on a spectral method in which the time-dependent electronic wavefunction is expanded in terms of a superposition of field-free eigenstates. The latter are the result of a configuration interaction (CI) calculation and thus include correlation. This, sometimes called spectral approach (in contrast to grid techniques), has proven its capabilities in the context of atomic calculations [17] as well as recently also for H_2^+ [18]. Although a variation of the internuclear distance and even a different orientation of the molecule with respect to the polarization of the laser field can be considered with the present method almost without modifications (and first calculations along these lines have actually already been performed), the present work concentrates mainly on results obtained for a fixed internuclear distance (the equilibrium distance of $R = 1.4a_0$, where a_0 is the Bohr radius) and a parallel orientation of a linearly polarized laser field and the molecular axis. The main intention of this paper is to demonstrate the correctness of the numerical implementation. This is done by comparing for very small internuclear distances to helium results and for low-intensities to LOPT predictions. The onset of non-perturbative behaviour is then demonstrated for higher intensities. The validity of the single-active electron (SAE) approximation is briefly discussed. The latter model is important, since it may be a valuable approach for extending the method to systems with more than two electrons while pertaining the explicit time dependence, as has been done for atoms. Finally, the ability of obtaining photoelectron spectra (including the above-threshold ionization ATI) is also shown.

2. Method

The three-dimensional TDSE is solved by expanding the time-dependent wavefunction in terms of field-free states. They are obtained from a CI calculation in which the Slater determinants are formed with the aid of H_2^+ wavefunctions expressed in terms of B splines in prolate spheroidal coordinates ($1 \leqslant \xi < \infty, -1 \leqslant \eta \leqslant 1, 0 \leqslant \phi < 2\pi$). The electronic structure CI method is discussed in detail in [19]. Note, electron–electron interaction is not included in the orbitals used for the CI calculation. Such an approach is especially suitable for asymmetric exited states (for example, a state where one electron is left in the lowest lying orbital while the other is ionized), but is not perfect for describing, e.g., the (symmetric) electronic ground state. Nevertheless, it has been shown in [19] that with the present approach very accurate ground-state energies can be obtained for H_2, if the basis set is chosen judiciously. In calculations as they are discussed here, a compromise has to be searched for, since the goal is to achieve a rather uniform accuracy with respect to the description of a plethora of states, from the ground state up to very energetic continuum ones.

A key feature of the approach is the discretization of the electronic continuum. This is a consequence of the chosen B-spline basis confined within a finite spatial volume defined by

$\xi_{\max}$. Therefore, only states that are confined within this volume or that have a node at the volume boundary are obtained (see [19] for a more detailed discussion). Since the code allows the calculation of the electronic states of any symmetry (singlet, triplet, Σ, Π, etc), it is also possible to perform calculations for any possible orientation of the molecular axis with respect to the polarization of the laser field. The use of the prolate spheroidal coordinate system allows the solution of the electronic problem for arbitrary values of the internuclear distance. This is an important advantage over the one-centre approximation. The latter was extensively used for H_2 in theoretical photoionization studies by Martín and collaborators (for a review see [20]). Also previous multiphoton studies on H_2 within LOPT adopted that approach [10]. However, the one-centre expansion converges very slowly for large internuclear distances.

The solution of the TDSE describing molecular hydrogen exposed to a laser field follows closely the approach that has successfully been used for one- and two-electron atoms before (see [17] for a review). The total in-field Hamiltonian is given by

$$\hat{H} = \hat{H}_0 + \hat{D}(t) \tag{1}$$

where $\hat{H}_0$ is the field-free electronic Born–Oppenheimer Hamiltonian of a hydrogen molecule and $\hat{D}(t)$ is the operator describing its interaction with the (time-dependent) laser field. The non-relativistic approximation is used for both operators, and the interaction is described within the dipole approximation and in velocity gauge, $\hat{D}(t) = -\mathbf{A}\cdot\mathbf{p}/c$. (Here and in the following atomic units ($e = m_e = \hbar = 1$) are used unless specified otherwise.) $\mathbf{A}$ is the vector potential of the laser field, $\mathbf{p}$ is the total momentum operator of the electrons and c is the velocity of light in vacuum. The resulting TDSE

$$\mathrm{i}\frac{\partial}{\partial t}\Psi = \hat{H}\Psi \tag{2}$$

is solved by expanding the wavefunction Ψ according to

$$\Psi(t) = \sum_{nL} b_{nL}(t)\phi_{nL} \tag{3}$$

in terms of the time-independent wavefunctions ϕ_{nL}. The latter are solutions of the field-free molecular Schrödinger equation

$$\hat{H}_0\,\phi_{nL} = E_{nL}\,\phi_{nL}. \tag{4}$$

The compound index L represents the total angular momentum (Σ, Π, ...) and the symmetry *gerade* or *ungerade*, in the case of Σ symmetry also + and −. The n is just an index of a state with the particular symmetry L. Due to the chosen approach for solving equation (4) (using a CI expansion based on H_2^+ orbitals that are expanded in a B-spline basis contained in a finite box) all states are discretized as was mentioned before. Therefore, the index n remains discrete even for states in the electronic continuum.

Substitution of equation (3) into the TDSE (equation (2)), multiplication of the result by ϕ^*_{mK} and integration over the electronic coordinates yields

$$\mathrm{i}\frac{\partial}{\partial t}b_{mK}(t) = E_{mK}b_{mK}(t) + \sum_{nL} D_{mK,nL}(t)b_{nL}(t) \tag{5}$$

with $D_{mK,nL}(t) = \langle\phi_{mK}|\hat{D}(t)|\phi_{nL}\rangle$. It should be emphasized that with this approach the complete time dependence is incorporated into the coefficients b_{nL}. They are calculated by propagating equation (5) numerically in time using a variable-order, variable-step Adams solver for ordinary first-order differential equations. The laser-pulse parameters are contained in $D_{mK,nL}(t)$. Different choices for the temporal shape of the pulse are implemented, but in this work only results obtained for $\cos^2$-shaped pulses (with respect to the vector potential $\mathbf{A}(t)$) are shown.

In order to compare the results of the TDSE calculations with those obtained within LOPT, it is required to convert the rates or generalized cross-sections of LOPT to excitation or ionization yields. As is, e.g., discussed in [10], the ionization rate $\Gamma^{(N)}$ in LOPT may be obtained from the generalized N-photon ionization cross-section $\sigma^{(N)}$ using

$$\Gamma^{(N)} = \sigma^{(N)} \left(\frac{I}{\hbar\omega} \right)^N \tag{6}$$

where $\Gamma^{(N)}$ is given in s^{-1}, $\sigma^{(N)}$ in $cm^{2N}\ s^{N-1}$, the laser intensity I in W cm^{-2} and the photon energy $\hbar\omega$ in Joule. Integration of the rate over the temporal pulse envelope gives the ionization yield

$$P_{\text{ion}} = \int_{\text{Pulse}} \Gamma^{(N)}\, \mathrm{d}t. \tag{7}$$

An interesting question in the field of laser-matter interaction is the importance of multi-electron effects. In other words, is the laser-induced single ionization process basically a single-electron process as is suggested by simple ionization models such as ADK or SFA? A strict SAE model would require to fix all electrons except the ionized one in their respective field-free orbitals and to use a single-determinant (correlation-free) description for all states. A natural choice for the orbitals would be Hartree–Fock orbitals. (Alternatively, all but the ionized electron are described by some pseudo or model potential.) In the present implementation the used orbitals do, however, not contain any electron–electron interaction, as is discussed above. These orbitals do not provide a very reasonable description of the remaining (non-ionized) electrons *before* the ionization process takes place. (However, they are in the present case of two-electron systems a very good description of the remaining ion after the ionization process, since they include relaxation completely.) The use of a Hartree–Fock orbital would on the other hand lead to non-orthogonality and a very asymmetric description of the two electrons. Thus, a version of the SAE is used in this work that partly contains two-electron effects. In this approach (see also [17] where it is discussed for atoms) only configurations where one electron is fixed in the lowest ionic orbital are included in the CI calculation. Although this implementation of the SAE contains correlation to a certain extent, the numerical efforts are still greatly reduced compared to the full CI approach. This is of very practical importance, since SAE calculations of this type are also feasible for more complicated molecules, at least diatomic molecules with more than two electrons.

In the present work, converged results were obtained using along the ξ coordinate 280 B splines of order $k = 15$ with a linear knot sequence. In the case of helium the box size (defined implicitly by $\xi_{\max}$ that depends on R) corresponds to $200a_0$, for H_2 to $196a_0$. Along the η coordinate 24 B splines of order 8 were used in the complete interval $-1 \leqslant \eta \leqslant +1$, but using the symmetry of a homonuclear system as is described in [19]. In the helium calculation the number of B splines was 240 along ξ and 24 along η. In most of the subsequent CI calculations approximately 3000 configurations were used for both the $^1\Sigma_g$ and the $^1\Sigma_u$ states. These states result from very long series (about 2000 configurations) where one electron occupies the H_2^+ ground-state $1\sigma_g$ orbital while the other is occupying one of the remaining $n\sigma_g$ or $n\sigma_u$ orbitals. The other configurations represent doubly excited situations and are responsible for describing correlation (and physical doubly excited states). For obtaining the photoelectron spectra a larger CI expansion was used that consists of about 5100 configurations out of which about 3300 are singly excited ones. The latter configurations were also used for obtaining the results within the SAE. In the helium calculation a similar selection of configurations was chosen despite the difference in the one-electron basis set. For the TDSE calculations an energy cut-off was used as an additional parameter. Only CI states with an energy below this cut-off (in the present case set to about 300 eV) were included in the time propagation.

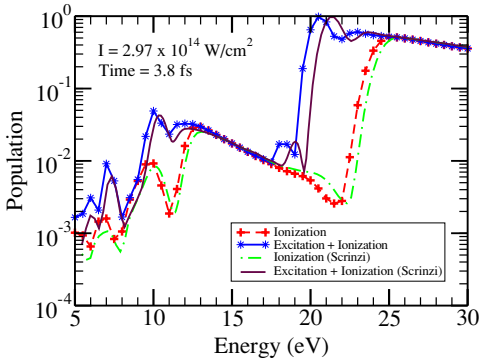

Figure 1. Calculated ionization yields (plus) and the sum of ionization and excitation to electronic bound states (stars) are shown as a function of the photon energy. The calculation was performed for a very small internuclear distance $R = 0.001a_0$ and thus simulates atomic helium. The results are compared to the atomic calculations performed by Scrinzi *et al* [21] (ionization: chain, sum of ionization and excitation: solid.)

3. Results

In order to test the new code it was first applied to helium for which accurate theoretical results exist. For this purpose the internuclear distance was reduced to a very small value ($R = 0$ leads to a breakdown of the adopted prolate spheroidal coordinate system), since in the united-atom limit H_2 corresponds to He, if the nuclear repulsion term is omitted. The calculated energies and dipole moments became practically independent of R for $R < 0.001a_0$. The population of continuum states (ionization yield) is shown as a function of the photon energy in figure 1 for a pulse length of 3.8 fs, a $\cos^2$ envelope for the vector potential ($\mathbf{A}$(t)) and the peak intensity $I = 2.97 \times 10^{14}$ W cm^{-2}. Also shown is the sum of the ionization yield and the population of all bound electronically excited states of neutral He. This is equal to $1 - P_{gs}$ where P_{gs} is the population left in the electronic ground state. These quantities have been reported (for the given laser parameters) in [21]. In that work explicitly correlated basis functions (geminals) had been adopted for calculating the field-free helium states. A good agreement is found between the two approaches, except that the present results are shifted to smaller energies with respect to the literature data. This shift is due to the inaccuracy in our ground-state energy and the correspondingly underestimated ionization potential. Although it has been shown that the present code allows for very accurate ground-state calculations [19], this requires a very judicious choice of the basis set. Such a basis set (requiring for a reasonable number of B splines the use of a small box) is, however, not optimal for the present purpose of describing a manifold of states, including the electronic continuum (requiring a large box). This problem is also discussed in [22] where an atomic B-spline based CI code is used. In fact, when comparing to the results in [22] there is almost perfect agreement. Besides the energy shift, the present calculation reveals all features found in [21], including the different multiphoton thresholds and the dip at about 20 eV caused by Rabi oscillations.

As is apparent from equation (6) inserted into equation (7), the intensity dependence of the ionization yield should be given by I^N, if the conditions for the validity of LOPT are fulfilled. If the ionization yield is plotted as a function of the laser peak intensity on a double logarithmic scale, the slope should be equal to N, the number of photons needed for ionization. In figure 2, such a plot is shown for three different photon energies. For 10 eV, 6.2 eV and 5.0 eV photons respectively 2, 3 and 4 photons are needed for reaching beyond the

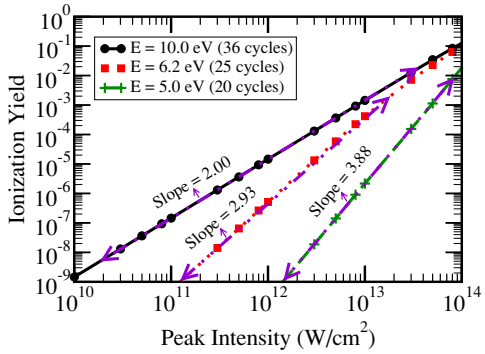

Figure 2. Ionization yield as a function of the laser (peak) intensity for three different photon frequencies (10 eV (circles, 14.88 fs), 6.2 eV (squares, 16.68 fs) and 5.0 eV (plus, 16.54 fs)). According to LOPT, the slope of the yield curve should be proportional to the number of photons needed for ionization, if plotted on a log–log scale. A slope of 2.0 for 10.0 eV, 2.93 for 6.2 eV and 3.88 for 5.0 eV is found.

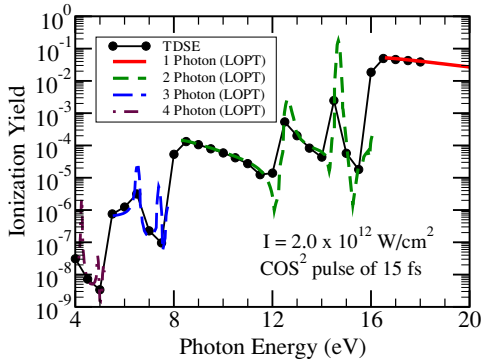

Figure 3. The ionization yield of H_2 as a function of the photon energy for a peak intensity of 2.0×10^{12} W cm^{-2} calculated within LOPT (solid and dashed lines) is compared to the full solution of the TDSE (circles).

ionization threshold (within the fixed-nuclei approximation). In order to achieve a comparable pulse length, the number of cycles varies for the shown photon frequencies between 20 and 36. Clearly, the intensity dependence follows in principle that expected from LOPT. On the logarithmic plot, the intensity dependence is strictly linear for a very large range of laser (peak) intensities (covering four orders of magnitude) and a change of the ionization yield by up to eight orders of magnitude. The slope of the curves is 2.00, 2.93 and 3.88 compared to the values 2, 3 and 4 predicted by LOPT. Clearly, the agreement in slope is not perfect. However, an overestimation of the slope by the LOPT is a fact that was found theoretically and experimentally already for atoms (see [23] and references therein).

In figure 3, the ionization yields calculated in the LOPT are compared with those obtained by a full solution of the TDSE. The laser-pulse parameters are given by a peak intensity of 2.0×10^{12} W cm^{-2} and a pulse length of 15 fs. A pronounced dependence of the ionization yield on the photon frequency is visible. In general, a good agreement is found between the LOPT results and the full TDSE solution. At the multiphoton ionization thresholds, the LOPT results are discontinuous while the TDSE calculation gives a sharp but continuous transition

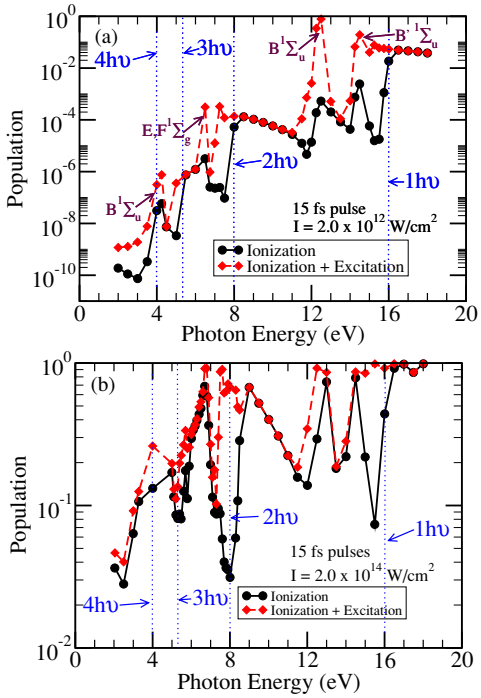

Figure 4. Ionization (circles) as well as the sum of ionization and excitation (diamonds) for H_2 as a function of photon energy for a 15 fs $\cos^2$ pulse ($\mathbf{A}(t)$) with peak intensities 2.0×10^{12} W cm^{-2} (a) and 2.0×10^{14} W cm^{-2} (b). Ionization thresholds are marked with vertical dotted lines. In (a) some intermediate resonances are identified and marked by arrows.

from one multiphoton regime (requiring N photons to reach the ionization threshold) to the neighbouring ones (requiring $N \pm 1$ photons). The shown range of photon energies covers the regime from one- to four-photon ionization ($N = 1$ to 4). The resonances are also more pronounced in the LOPT spectra. This is due to the finite bandwidth of the Fourier-transform limited short pulse (and possible power broadening) included in the TDSE calculation but absent in (simple) LOPT. In fact, the LOPT calculation diverges at the resonances and thus the height of the resonances calculated with LOPT is arbitrary. Of course, it is in principle possible to correct also the LOPT spectra by incorporating a finite bandwidth of a realistic laser, but this is beyond the scope of the present work.

In figure 4(a), the ionization yield is shown together with the sum of ionization and excitation as a function of the photon energy (for the same pulse parameters as in figure 3). This graph allows us to discuss the spectra in more detail. For this purpose also the respective multiphoton ionization thresholds are marked (by vertical lines). The given values correspond to the results (ground-state energies of H_2 and H_2^+ at the internuclear distance $R = 1.4a_0$) obtained with the present calculation. As has been discussed in the case of the helium results before, those values underestimate the correct values due to the limited accuracy of the ground-state energy of H_2 as obtained with the chosen basis set. It may be noted that the physical ionization threshold (beyond the present frozen-nuclei approximation) is on the other hand even smaller than that shown.

For photon energies larger than about 16.1 eV, a single photon is sufficient for ionization. Thus, the laser-molecule interaction is dominated by direct single-photon ionization without

excitation of bound states. Below the one-photon threshold ionization occurs as a two-photon process. However, close to the threshold (just below 16 eV) two-photon ionization competes with single-photon excitation of electronic Rydberg states. The latter process is clearly dominant. At about 12.5 eV and 14.5 eV, the ionization yield is strongly enhanced. As is evident from the summed excitation and ionization curve, the ionization is resonantly enhanced, i.e. one has a resonantly enhanced two-photon (1+1) ionization process (REMPI) via the $B\,^1\Sigma_u$ and the $B'^1\Sigma_u$, respectively. Again, the population of these excited states dominates clearly over the ionization process. For the given laser-pulse parameters, the $B\,^1\Sigma_u$ transition is in fact almost completely saturated.

In between 11 eV and the three-photon threshold at 8.0 eV, one photon is insufficient to excite any bound state, and thus only non-resonant two-photon ionization (without excitation of bound states) is observed in this photon-energy regime. Similar to the situation at 16 eV, the ionization yield drops by more than two orders of magnitude, once the photon energy is insufficient for two-photon ionization and thus three-photon ionization has to occur. The sum of ionization and excitation (and thus the depopulation of the ground state) remains (again similar to the situation at 16 eV) almost constant at photon energies just below the two-photon threshold. This indicates that the excitation of the Rydberg states (by two-photon absorption) occurs with a comparable probability as two-photon ionization. In view of the structural similarity of high-lying Rydberg states with the low-energy continuum (being also responsible for the success of quantum defect theories) this is not surprising. Around 6.5 eV the ionization yield is again resonantly enhanced. This time a (2+1) REMPI process proceeding via two-photon excitation of the E, $F\,^1\Sigma_g$ state (positioned around 13.0 eV above the electronic ground state) is responsible. While the three-photon absorption to the $B\,^1\Sigma_u$ state (at 4 eV) is clearly visible, the corresponding (3+1) REMPI process is almost hidden by the occurrence of the four-photon ionization threshold. A higher energy resolution would be required in this low photon-energy regime for a more detailed discussion. However, the disappearance of pronounced structures in the low photon-energy regime is also due to physical reasons. With an increase of the number of photons involved in the absorption process, the different multiphoton thresholds approach each other. For a fixed pulse length (as in figure 3) the *relative* bandwidth thus becomes broader. This effect tends to wash out the details of the spectrum for lower photon energies.

In figure 4(b), the results obtained for the higher peak intensity 2.0×10^{14} W cm^{-2} are shown. Expectedly, the overall ionization yield is dramatically increased due to the increase of the peak intensity by two orders of magnitude. As a result of saturation and the large ionization rate of the $B'^1\Sigma_u$ state in a high-intensity field, the (1+1) REMPI process dominates at around 14.5 eV. In the case of the $B\,^1\Sigma_u$ state the situation is slightly different. While a behaviour similar to that of the $B'^1\Sigma_u$ state is found at the high-energy side of the resonance, excitation dominates over ionization on the low-energy side. There are two differences between the two resonant states that may be responsible for the different behaviour. Only the B state is well isolated from other (dipole-allowed) states within the bandwidth of the laser, while the B′ state overlaps with the higher lying Rydberg states. Also the ionization rate of the B′ state is expected to be larger than that of the B state, due to the difference in ionization potential. (Note, however, that it has been discussed previously [24] that these simple arguments do not necessarily apply to non-isolated excited states.) In the case of the (2+1) REMPI at 6.5 eV (E, F state) ionization and excitation are also of similar order of magnitude, the former being now dominant in contrast to the case of lower intensity.

The multiphoton ionization thresholds indicated in figure 4(b) correspond to their field-free values. Clearly, the drop in the ionization yield when going, e.g., from the two- to the three-photon regime (around 8 eV) occurs at a higher photon frequency than one would expect

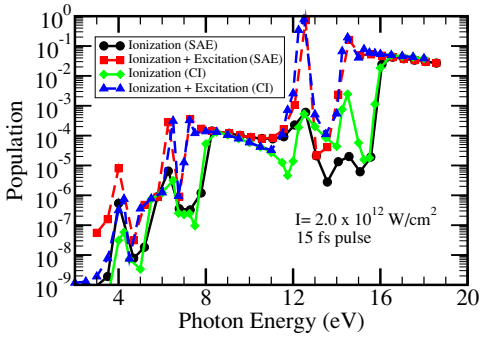

Figure 5. Comparison of the TDSE results obtained with the CI approach and within the single-active electron approximation (SAE, defined in the text). The results of the SAE are corrected for the difference in ionization potential compared to the CI calculation. The ionization yield (solid) and the sum of ionization and excitation yield (dashed) are shown as a function of photon energy.

on the basis of the field-free multiphoton ionization threshold. This is easily understood by considering the ponderomotive shift $U_p = I/4\omega^2$ where I is the intensity of the laser and ω the photon frequency. For the given peak intensity and a photon energy of 8 eV, this ponderomotive shift amounts to about 0.45 eV. The ionization threshold shifts correspondingly. As a result, for a fixed photon energy, a decrease of the ionization yield is observed for energies very close to a multiphoton ionization threshold. This is the well-known effect of channel closing. Since the ponderomotive shift increases with decreasing photon energy, this effect is even more pronounced for the higher multiphoton thresholds. However, at some point the different intensity-related effects (power broadening etc) lead to a loss of spectral details. At the same time the relative importance of the order of the multiphoton process decreases with the number of photons involved, i.e. the N and $N \pm 1$ transition amplitudes are not too different, if both N and the intensity are large. This high-intensity and low photon-frequency limit is of course the tunnelling (or over-the-barrier) ionization regime in which the ionization process is (almost) photon-energy independent. The Keldysh parameter $\gamma = \sqrt{I_p/2U_p}$ (with the ionization potential I_p) is supposed to indicate the transition from the multiphoton to the tunnel regime. Its value approaches 1 at the lowest photon energy shown in figure 4(b). Therefore, one would expect the shown low-energy results to represent neither simple multiphoton ionization (as predicted by LOPT) nor pure tunnelling. This is the non-perturbative multiphoton regime where full TDSE solutions are expected to be most important, even in those cases where the shortness of the laser pulse does not play a role.

Using the same pulse parameters as in figure 4(a) the results obtained within the SAE approximation are compared with the full calculation in figure 5. Again the ionization yield is shown together with the sum of ionization and excitation. Since the ground-state energies of H_2 obtained with SAE or CI differ from each other, the SAE results are shifted. Above 8 eV, an energy shift of 0.57 eV is applied. This corresponds to the difference between the H_2 SAE and CI ground-state energies. Between 5.33 and 8.0 eV a shift of 0.285 eV (half the ground-state energy difference) and between 4.0 and 5.33 eV a shift of 0.19 eV (one third of the energy difference) are used. The agreement between SAE and the full calculation is reasonably good in the non-resonant regimes (8.5 eV to 10.5 eV and above 16.0 eV). At low photon energies the quantitative agreement is not good, but still SAE reproduces most of the qualitative features correctly. These findings agree with those found earlier for atomic systems. In view of the denser level structure in molecules compared to atoms due to the

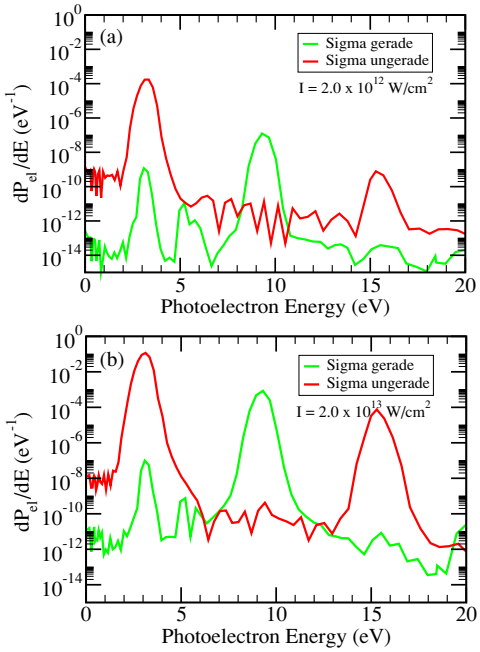

Figure 6. Energy-resolved photoelectron spectrum of H_2 after exposure to a laser pulse with photon energy 6.2 eV, length of 25 cycles and peak intensities 2.0×10^{12} W cm^{-2} (a) or 2.0×10^{13} W cm^{-2} (b). The population of $^1\Sigma_g$ and $^1\Sigma_u$ final states are shown separately.

additional rovibrational degrees of freedom, the applicability of the SAE to molecules may, however, be more problematic than for atoms. This effect of dense resonant structure is of course not accounted for in the present fixed-nuclei calculation, but should be investigated more carefully in the future.

In figure 6, the energy-resolved photoelectron spectra are shown for pulses with peak intensities 2×10^{12} W cm^{-2} and 2×10^{13} W cm^{-2}. The photon energy is 6.2 eV and the pulse contains 25 cycles. The photoelectron spectra corresponding to different symmetries ($^1\Sigma_g$ and $^1\Sigma_u$) of the complete system $H_2^+ + e^-$ are given separately, but have to be added for a comparison to experiment. Within the adopted fixed-nuclei approximation, the shown energy range corresponds up to about 18.9 eV to the situation where H_2^+ is left in its electronic ground state ($X\ ^2\Sigma_g$). The symmetry of the complete system reflects therefore the symmetry of the photoelectron distribution. For higher energies a multichannel situation arises, since H_2^+ may also be left in one of its electronic excited states. Solutions for treating the multichannel problem (using box-discretized approaches) have been discussed in the literature and a corresponding implementation is a future task. As is discussed in [19], in the molecular case there exists a multichannel problem even below the first excited state of the ion. The solution discussed there (based on an analysis of the leading channel of a given state and a subsequent density-of-states normalization) is also adopted here.

Although it has been shown above that for the pulse parameters in figure 6(a), LOPT gives very accurate results for the total ionization rate, non-perturbative effects are nevertheless visible from the energy-resolved spectrum. According to LOPT a photon energy of 6.2 eV corresponds to three-photon ionization. Therefore, the dipole selection rule allows only for final states with $^1\Sigma_u$ symmetry. Figure 6(a) shows on the other hand that the population of

$^1\Sigma_g$ states is small, but clearly non-zero. In fact, LOPT takes only into account the energy conserving three-photon transition and thus only the first peak. Especially the other (so-called ATI) peaks (implying the absorption of more than the minimum number of photons necessary to reach the ionization continuum) are not present in standard LOPT. The key feature for the validity of LOPT with respect to the total ionization rate is the dominance of the first peak that for the laser parameters in figure 6(a) accounts almost exclusively for the total ionization rate. This is a good example for cases where a simpler model (here LOPT) may be able to quantitatively correctly reproduce integrated observables like the total ionization yield, but still may not be capable of describing a differential observable (here the photoelectron spectra) even qualitatively.

Increasing the intensity to 2×10^{13} W cm^{-2} results, of course, in a larger total ionization yield, but also changes the shape of the photoelectron spectrum. For higher intensities the relative contribution of the ATI peaks to the total ionization yield increases. While for the lower laser intensity shown in figure 6(a) the height of the second ATI peak is about five orders of magnitude smaller than the fundamental peak, it is only three orders of magnitude for the ten times higher laser intensity in figure 6(b). As a consequence, an increasing intensity requires to take into account an increased number of ATI peaks in order to obtain the correct ionization yield. Even the higher laser peak intensity in figure 6(b) corresponds according to the Keldysh parameter ($\gamma \approx 10$) still to the multiphoton regime. The fact that the photoelectron spectrum is dominated by well-defined peaks separated by the photon energy is a clear demonstration of the dominating photon character of the interaction of such a laser field with H_2. Nevertheless, the non-zero background photoelectron spectrum indicates the fact that even for the given values of Keldysh parameters there is some strong-field ionization occurring that reflects the field character of the photons. Its contribution to the total ionization yield is, however, completely negligible.

4. Conclusion and outlook

On the basis of a recently developed *B*-spline-based CI code for two-electron diatomic molecules, a numerical approach for solving the TDSE of a hydrogen molecule exposed to a short intense laser pulses was developed. The implementation is presently limited to the fixed-nuclei approximation, but an arbitrary variation of the internuclear distance is possible. Even an arbitrary orientation of the molecular axis relative to the laser polarization can be considered by the present approach, an important advantage to the only so-far existing other fully three-dimensional correlated approach based on a grid.

The proper implementation of the code is demonstrated by comparing results obtained for extremely small internuclear distances with those of a very accurate calculation describing atomic helium exposed to ultrashort laser pulses. A second test comprises a comparison to the prediction of LOPT that should be applicable for sufficiently low intensities. Increasing the peak intensity of the laser then shows first deviations from the behaviour predicted by LOPT, mainly due to the power broadening of resonant transitions and the ponderomotive shift leading to channel closing. While these conclusions are valid for the total ionization yield, the analysis of the energy-resolved continuum population (corresponding to the photoelectron spectrum within the first two ionization thresholds) reveals even for the lower intensities the importance of non-perturbative effects. This indicates not only the importance of experiments yielding differential observables, but also the need to compare the predictions of different theoretical models on more detailed quantities than the total ionization yield.

Future work that is already partly started includes a discussion of the *R* dependence of the ionization rate and its consequences for, e.g., the expected vibrational distribution of H_2^+ formed

in laser-pulse ionization of H_2. Another important aspect of the current work in progress is the orientational dependence of the ionization rate. In both cases, a comparison to simplified models such as (MO-)ADK or SFA is certainly of great interest. Another simplified (though more complicated) model is the SAE approximation. The present work already discussed some aspects of this model that may be a good starting point for applying the present approach to more complicated systems, i.e. to multielectron diatomics. Although a future goal of the present work is the full incorporation of nuclear motion, it should be realized that especially for very short pulses (as they are presently becoming available) the nuclei may in fact be treated as frozen during the pulse duration. This indicates the importance of the present approach already in its present stage for understanding H_2 in ultrashort pulses.

Acknowledgments

The authors acknowledge financial support by the *Deutsche Forschungsgemeinschaft* (DFG-Sa 936/2). AS is grateful to the *Stifterverband für die Deutsche Wissenschaft* (Programme *Forschungsdozenturen*) and the *Fonds der Chemischen Industrie* for financial support. This work is also supported by the European COST Programme D26/0002/02.

References

[1] Hentschel M, Kienberger R, Spielmann C, Reider G A, Milosevic N, Brabec T, Corkum P, Heinzmann U, Drescher M and Krausz F 2001 *Nature* **414** 509
[2] Paul P, Toma E, Breger P, Mullot G, Augé F, Balcou P, Muller H and Agostini P 2001 *Science* **292** 1689
[3] Kitzler M, Milosevic N, Scrinzi A, Krausz F and Brabec T 2002 *Phys. Rev. Lett.* **88** 173904
[4] Carr G L, Martin M C, McKinney W R, Jordan K, Neil G R and Williams G P 2002 *Nature* **420** 153
[5] Bartels R, Backus S, Zeek E, Misoguti L, Vdovin G, Christov I P, Murnane M M and Kapteyn H C 2000 *Nature* **406** 164
[6] Posthumus J H 2005 *Rep. Prog. Phys.* **67** 623
[7] Tong X M, Zhao Z X and Lin C D 2002 *Phys. Rev.* A **66** 033402
[8] Tong X M, Zhao Z X and Lin C D 2003 *Phys. Rev. Lett.* **91** 233203
[9] Urbain X, Fabre B, Staicu-Casagrande E M, de Ruette N, Andrianarijaona V M, Jureta J, Posthumus J H, Saenz A, Baldit E and Cornaggia C 2004 *Phys. Rev. Lett.* **92** 163004
[10] Apalategui A and Saenz A 2002 *J. Phys. B: At. Mol. Opt. Phys.* **35** 1909
[11] Becker A and Faisal F H M 2005 *J. Phys. B: At. Mol. Opt. Phys.* **38** R1
[12] Muth-Böhm J, Becker A and Faisal F H M 2000 *Phys. Rev. Lett.* **85** 2280
[13] Kjeldsen T K and Madsen L B 2005 *Phys. Rev.* A **71** 023411
[14] Chelkowski S, Foisy C and Bandrauk A D 1998 *Phys. Rev.* A **57** 1176
[15] Niikura H, Villeneuve D M and Corkum P B 2005 *Phys. Rev. Lett.* **94** 083003
[16] Harumiya K, Kono H, Fujimura Y, Kawata I and Bandrauk A D 2002 *Phys. Rev.* A **66** 043403
[17] Lambropoulos P, Maragakis P and Zhang J 1998 *Phys. Rep.* **305** 203
[18] Barmaki S, Bachau H and Ghalim M 2004 *Phys. Rev.* A **69** 043403
[19] Vanne Y V and Saenz A 2004 *J. Phys. B: At. Mol. Opt. Phys.* **37** 4101
[20] Martín F 1999 *J. Phys. B: At. Mol. Opt. Phys.* **32** R197
[21] Scrinzi A and Piraux B 1998 *Phys. Rev.* A **58** 1310
[22] Lambropoulos P, Kornberg M A, Nikolopoulos L A A and Saenz A 2000 *Multiphoton Processes* ed L F DiMauro, R R Freeman and K C Kulander (New York: Melville) p 231
[23] Maragakis P, Cormier E and Lambropoulos P 1999 *Phys. Rev.* A **60** 4718
[24] Saenz A 2002 *J. Phys. B: At. Mol. Opt. Phys.* **35** 4829